MIT Open Access Articles

Analytical Solutions for Multicomponent, Two-Phase Flow in Porous Media with Double Contact Discontinuities

Analytical Solutions for Multicomponent, Two-Phase Flow in Porous Media with Double Contact Discontinuities

C. J. Seto[*] and F. M. Orr Jr.

Department of Energy Resources Engineering, Stanford University, Stanford CA 94305, USA.

[*] Corresponding author. Now with the MIT Energy Initiative, Massachusetts Institute of Technology, Department of Chemical Engineering, 77 Massachusetts Avenue, Room 66-060, Cambridge MA 02141, USA. e-mail: cjseto@mit.edu

Abstract

This paper presents the first instance of a double contact discontinuity in analytical solutions for multicomponent, two-phase flow in porous media. We use a three-component system with constant equilibrium ratios and fixed injection and initial conditions, to demonstrate this structure. This wave structure occurs for two-phase injection compositions. Such conditions were not considered previously in the development of analytical solutions for compositional flows. We demonstrate the stability of the double contact discontinuity in terms of the Liu entropy condition and also show that the resulting solution is continuously dependent on initial data. Extensions to four-component and systems with adsorption are presented, demonstrating the more widespread occurrence of this wave structure in multicomponent, two-phase flow systems. The developments in this paper provide the building blocks for the development of a complete Riemann solver for general initial and injection conditions.

Keywords: method of characteristics, Riemann problem, analytical solution, multicomponent flow, degenerate shock, double contact discontinuity, two-phase injection.

1. Introduction

The development of analytical solutions for the dispersion-free limit of multiphase, multicomponent flow using the method of characteristics (MOC) is a well established technique. This method has been applied to modeling many enhanced oil recovery strategies, ranging from multicontact miscible gas injection (Helfferich 1981, Johns and Orr 1996, Dindoruk *et al.* 1997), to surfactant and polymer flooding (Isaacson 1981, Hirasaki 1981, Johansen and Winther 1988) and enhanced coalbed methane recovery (Zhu *et al.* 2003, Seto *et al.* 2006). In all of these processes, the resident hydrocarbon is recovered through a complex interaction between phase behavior and multiphase flow. Application of this technique to analyzing injection processes has led to improved understanding of the physics of the recovery mechanism (Larson and Hirasaki 1978, Monroe *et al.* 1990, Orr *et al.* 1993, Johns and Orr1996, Jessen and Orr 2004, Juanes and Blunt 2007) and has contributed to the development of efficient tools for more accurate simulations of these processes (Lie and Juanes 2005, Seto *et al.* 2007, Juanes and Lie 2008).

In many of these applications, the boundary conditions are specified such that the injection and initial fluids are single phase. Under these particular conditions, a number of researchers have developed algorithms for determining the structure of the solution (Johns 1992, Jessen *et al.* 2001, Wang *et al.* 2005). Jessen and Orr (2004), LaForce and Johns (2005) and Seto *et al.* (2007) considered single-phase fluid injection into a system that initially contained two phases to model gas injection for condensate recovery. Solution structures from their analyses were similar to those found in single-phase injection and initial conditions, and algorithms for constructing solutions followed the same methodology.

Much of the MOC theory for multicomponent flow has focused on injection of single-phase mixtures (Monroe *et al.* 1990, Johns 1992, Dindourk 1992, Wang 1998, Jessen *et al.* 2001). Only recently, have researchers considered multiphase injection compositions (Seto 2007, LaForce and Jessen 2007). Although two-phase injection compositions have not been thoroughly investigated in gas displacements, they have been explored for immiscible three-phase flow (Falls and Schulte 1992, Guzman and Fayers 1997, Marchesin and Plohr 2001, Juanes and Patzek 2004, LaForce *et al.* 2008). Marchesin and Plohr (2001) demonstrated that two-phase injection can be understood as the limit of cyclic injection.

The algorithms developed for four-component (Monroe *et al.* 1990) and multicomponent systems (Jessen *et al.* 2001) identified n_c-1 key tie lines required, for constructing the solution. Once these were identified, a critical step in constructing the solution was to identify the shortest key tie line, as solution construction starts at that tie line. The solutions presented in this paper involve n_c key tie lines, and in the three-component example, solution construction is initiated at the longest key tie line. Another consequence of considering single-phase injection compositions only is that only one branch of the nontie-line composition path is utilized. The wave structure reported in this paper utilizes both branches of the nontie-line path.

This paper presents a solution structure in which a double contact discontinuity, involving two distinct genuine nonlinear characteristic families, plays a fundamental role. In this context of multicomponent, multiphase flow, this kind of discontinuity

has first appeared in the solution for a two-component, two-phase flow for a polymer flooding model (Johansen and Winther 1988). For a linearly degenerate characteristic field, this transitional contact discontinuity involving the slow and fast characteristic families have also been reported in a class of polymer models, known as the KK models (Keyfitz and Kranzer 1980, Isaacson 1981, Mota 1992, Souza 1995). In the context of a three-phase flow in porous media, a double contact discontinuity, but this time involving the same genuine nonlinear characteristic family (the fast family), was necessary to obtain the complete Riemann solution description for arbitrary initial and injection conditions (Isaacson *et al.* 1992, Souza 1992). Finally, this kind of discontinuity has been reported in other fields too, such as modeling sedimentation of polydispersive suspensions (Berres and Burger 2007).

The wave structure presented here provides the building block for obtaining analytical solutions with any initial and injection condition. The complete set of solutions for any injection and initial condition is of value because it allows the development of a Riemann solver which can be used to efficiently solve the system for any set of boundary conditions.

The structure of the paper is as follows. Section 2 presents the mathematical model for two-phase, multicomponent flow. Section 3 presents the double contact discontinuity that arises under two-phase injection in three-component systems. We also discuss the development and stability of this structure, and analyze the conditions under which it occurs. Extensions to four-component displacements and to systems with adsorption are given in Section 4. They demonstrate that the double contact discontinuity can arise in a variety of compositional flow settings. The main conclusions are summarized in Section 5.

2. Mathematical Model

The conservation equations for the dispersion-free limit of multicomponent, two-phase flow in 1D are (Helfferich 1981)

$$\frac{\partial C_i}{\partial t} + \frac{\partial F_i}{\partial x} = 0, \qquad i = 1, \ldots, n_c, \qquad (1)$$

where

$$C_i = x_i(1 - S) + y_i S, \qquad i = 1, \ldots, n_c, \qquad (2)$$

and

$$F_i = x_i(1 - f) + y_i f, \qquad i = 1, \ldots, n_c. \qquad (3)$$

C_i is the overall composition for component i, F_i is the overall fractional flow of component i, x_i is the liquid phase composition of component i, y_i is the vapor phase composition of component i, S is the vapor phase saturation and f is the vapor phase fractional flow. This model assumes the usual simplifications made in frontal advance theory (Helfferich 1981): 1D flow; homogenous and isotropic porous medium; negligible dispersive effects created by diffusion, dispersion, gravity and capillary forces; incompressible fluids; isothermal flow and instantaneous equilibrium as fluids mix as they propagate downstream. Extensions to Eqs. (1) to (3) to include adsorption and desorption effects are presented in Section 4.2.

Equations (1)-(3) are subject to the following constraints:

$$\sum_{i=1}^{n_c} C_i = 1, \qquad \sum_{i=1}^{n_c} x_i = 1, \qquad \sum_{i=1}^{n_c} y_i = 1. \tag{4}$$

Because F_i and C_i are dependent on phase behavior and saturation, the governing equations can be converted to an eigenvalue problem. The eigenvalues represent the characteristic wave propagation speeds of compositions through the displacement, and the corresponding eigenvectors are the directions of variation in composition space that satisfy the differential equations.

The Riemann problem consists of solving a system of conservation laws in an infinite domain, with piecewise-constant initial states separated by a single discontinuity. Continuous variation of the solution from the injection state to the initial state may result in non-monotonic variation of wave velocity, resulting in a multivalued state for a specific wave velocity. Such states are unphysical; therefore, additional constraints are needed to construct unique solutions: the velocity rule and an entropy condition (Isaacson 1981, Helfferich 1981).

The velocity rule specifies that faster-propagating states lie downstream of slower-propagating states. In situations where a continuous variation violates the velocity rule, a shock must be introduced to resolve the multivalued state. Shock segments are discontinuous, and therefore, the shock must satisfy the integral form of the conservation equation. This is achieved by applying the Rankine-Hugoniot condition. For each component, the integral balance across the shock is

$$\Lambda = \frac{F_i^L - F_i^R}{C_i^L - C_i^R}, \qquad \forall \quad i = 1, \ldots, n_c, \tag{5}$$

where Λ is the shock velocity and L and R represent conditions upstream and downstream from the shock.

The entropy condition ensures shock stability, requiring that the velocity immediately downstream of the shock be slower than the shock velocity, and the velocity immediately upstream of the shock be faster than the shock velocity. Under a small perturbation, the shock remains self-sharpening as it propagates through the displacement. If velocities on either side of the shock do not satisfy these requirements, the shock is unstable and collapses under a small perturbation.

In the solutions that follow, we assume that gas and liquid phase relative permeabilities are described by quadratic functions of saturation. As a consequence, the fractional flow is a function of saturation,

$$f = \frac{S^2}{S^2 + M(1 - S - S_{or})^2}, \tag{6}$$

where M is the ratio of vapor viscosity to liquid viscosity and S_{or} is the residual oil saturation, the saturation below which the liquid phase is immobile. The analysis presented in this paper assumes constant phase viscosities. Component partitioning between phases is described by the relations:

$$K_i = \frac{y_i}{x_i}, \qquad i = 1, \ldots, n_c, \tag{7}$$

where K_i is the equilibrium ratio (or K-value) for component i. Components are arranged in order of decreasing volatility, such that $K_1 > K_2 > \ldots > K_{n_c}$. In the section that follows, we assume that the K values are independent of composition.

3. Double Contact Discontinuity
3.1. Composition Paths

The developments in this paper rely on the MOC theory for compositional displacements (see Helferrich 1981, Dindoruk 1992, Johns 1992, Johansen *et al.* 2005, and references therein). The two families of eigenvalues and eigenvectors, can be classified into two types: one which follows the tie-line composition and is a function of saturation (tie-line eigenvalue, λ_t) and one which varies between the tie lines and is a function of both saturation and tie-line equilibrium composition (nontie-line eigenvalue, λ_{nt}). Setting S and x_1 as dependent variables,

$$\lambda_t = \frac{dF_1}{dC_1}, \qquad \lambda_{nt} = \frac{F_1 - \pi}{C_1 - \pi}, \qquad\qquad \text{(8 a, b)}$$

where

$$\pi = \frac{(K_1 - K_2)(K_1 - K_3)}{(K_2 - 1)(K_3 - 1)} x_1^2. \qquad\qquad \text{(9)}$$

The case of fixed mobility ratio, constant K-value, no volume change on mixing case admits closed form integration of the nontie-line path and is derived in Wang *et al.* (2005). Figure 1 shows the composition paths (tie-line and nontie-line paths) for a system with $K_1 = 2.8$, $K_2 = 1.5$, and $K_3 = 0.1$, and $M = 0.5$ and $S_{or} = 0$. For each tie line, there are two points where the nontie-line path is tangent to the tie-line path, and the eigenvalues are equal. At these points, the eigenvalues switch from a situation where the tie-line path is the fast path and the nontie-line path is the slow path to a situation where the ordering is reversed. Therefore, the system is nonstrictly hyperbolic (Dafermos 2005). The equal-eigenvalue points correspond to inflection points on the nontie-line path where one corresponds to a minimum, λ_{nt}^{min}, and the other corresponds to a maximum, λ_{nt}^{max}. Figure 2 shows the evolution of characteristic speeds along a tie line. Characteristics in the two-phase region can be mapped into three regions defined by the λ_{nt}^{min} and λ_{nt}^{max} loci:

- $S_g(0) < S_g\left(\lambda_{nt}^{min}\right)$: λ_{nt} is the fast path, and λ_{tl} is the slow path,
- $S_g\left(\lambda_{nt}^{min}\right) < S_g\left(\lambda_{nt}^{max}\right)$: λ_{nt} is the slow path, and λ_{tl} is the fast path, and
- $S_g\left(\lambda_{nt}^{max}\right) < S_g(1)$: λ_{nt} is the fast path, and λ_{tl} is the slow path.

3.2. Wave Structures in Three-Component, Two-Phase Flow
Before describing the double contact discontinuity that appears for two-phase injection conditions, we recall the traditional construction of analytical solutions for single-phase injection (Monroe *et al.* 1990, Orr 2007). The composition path and solution profile are presented in Figures 3 and 4. We consider injection of pure C_1 (I_1) to displace a mixture of 0.4 C_2 and 0.6 C_3 (O). All compositions are reported in overall mole fractions. We identify the initial tie line as the shortest tie line and initiate solution construction from that tie line. The solution starts with a phase change shock along the initial tie line from initial conditions into the two-phase region (O to A). This is followed by a tie-line rarefaction to the equal-eigenvalue point (A to B). At the equal-eigenvalue point, there is a path switch from the tie-line path to the

nontie-line path. A nontie-line rarefaktion connects the initial tie line to the injection tie line (B to C_1). At point C_1, the landing point of the nontie-line path on the injection tie line, there is a path switch from the nontie-line path to the tie-line path, which corresponds to a zone of constant state in the solution profile. This is followed by a phase change shock along the tie line out to the injection conditions at I_1 (C_1 to I_1).

The double contact discontinuity solution is compared to the previously described composition route in Figures 3 and 4. We consider the injection of a mixture of 0.594 C_1 and 0.406 C_3 (I_2) to displace a mixture of 0.4 C_2 and 0.6 C_3 (O). The solution path starts with a shock from the initial composition into the two-phase region, along the initial tie line (O to A). At point A, the shock velocity $\left(\Lambda^{OA}\right)$ and the initial tie-line rarefaction velocity $\left(\lambda_t^A\right)$ coincide. This is followed by a tie-line rarefaction to the equal eigenvalue point (A to B). At the equal-eigenvalue point, the solution switches from the tie-line path to the nontie-line path. A nontie-line rarefaction extends only to an intermediate tie line (B to C_2), which is followed by a tie-line shock to another nontie-line path (C_2 to D). This is followed by a nontie-line rarefaction to the injection composition (D to I_2). There are three features of this solution that have not previously been reported: 1) partial use of the nontie-line branch emanating from the equal-eigenvalue point of the initial tie line, 2) use of an intermediate tie line, which we term the double contact tie line (C-tie line) and 3) utilization of the interior branch of the nontie-line path.

Although segments of this solution are present in the traditional construction, Figure 3, the intermediate tie line is required to complete the solution, resulting in a solution that requires n_c key tie lines, as opposed to the n_c-1 tie lines found in conventional solutions. Next, we analyze the four other possibilities for solution construction and demonstrate why they are not valid constructions.

The first possible solution is a shock along the injection tie line from injection composition to the landing point of the nontie-line path from the initial tie line on the injection tie line (I to C). This path is shown in Figure 5. This is the solution that follows the traditional construction (Dindoruk 1992). It is inadmissible because the IC shock velocity is larger than the nontie-line wave velocity at C:
$1.0756 = \Lambda^{IC} > \lambda_{nt}^C = 1.0487$. Therefore, the velocity rule is violated.

Next we consider a tie-line shock from the injection composition to the landing point of the interior branch of the nontie-line path from the initial tie line (I to C), followed by a nontie-line rarefaction along to the initial tie line (C to B). Figure 6 shows composition path. This composition path is also inadmissible because the IC shock velocity is larger than the nontie-line wave velocity at C:
$2.0305 = \Lambda^{IC} > \lambda_{nt}^C = 1.0403$. Once again, the velocity rule is violated.

The third route is a shock from the injection tie line to another point on the nontie-line path (I to C), followed by a nontie-line rarefaction up to the initial tie line (C to B). Figure 7 shows the Hugoniot locus traced from the injection composition (I). The Hugoniot locus does not intersect the tie line of the initial composition. Therefore, a shock from injection composition to the initial tie line is not permissible. However, the Hugoniot locus does intersect the nontie-line path at point C, and a shock from the

injection state to a point on the nontie-line path is permissible:
$1.0760 = \Lambda^{IC} < \lambda_{nt}^C = 1.1205$. Although this shock obeys the velocity rule, it does not satisfy the 1-Lax entropy condition (Lax 1957), because the upstream nontie-line wave velocity is slower than the shock velocity: $1.0441 = \lambda_{nt}^I < \Lambda^{IC}$. Therefore, this solution is also inadmissible.

The final potential solution route makes use of the interior branch of the nontie-line path from the injection condition, I. While the wave velocities of this path increase towards the maximum, this branch is nested inside the nontie-line path tangent to the initial tie line (Figure 8). In other words, the nontie-line path passing through I does not intersect an admissible path emanating from O, and continuous variation from injection tie line to initial tie line is not possible. Therefore, a shock between the nontie-line branches is required to complete the solution structure. We now show that such a solution route is admissible.

Figure 9 shows how nontie-line eigenvalues vary as the nontie-line paths from point I on the injection tie line and from point B on the initial tie line are traced. There is one tie line between the injection and initial tie lines at which the two nontie-line eigenvalues are equal. A path switch between nontie-line branches is permissible there. A shock along this tie line is required to switch from the upstream nontie-line path to the downstream nontie-line path, because continuous variation along the tie line, from D to C, violates the velocity rule (Figure 10). This shock provides the transition between the slow and fast characteristic families. The shock velocity between states C and D satisfies

$$\lambda_{nt}^C = \Lambda^{CD} = \lambda_{nt}^D . \tag{10}$$

This type of shock is called a double contact discontinuity (Dafermos 2005) or a degenerate shock (Jeffrey 1976). The shock velocity coincides with the common characteristic velocity of both nontie-line branches. The sequence of compatible waves is shown in Figure 11. Because the velocities immediately upstream and downstream of the shock coincide with the shock velocity, there is no zone of constant state that connects the two nontie-line paths. The tie-line along which this occurs we call the contact tie line (C-tie line).

3.3. Stability of the Double Contact Discontinuity
The double contact discontinuity associated with the C-tie line is neither a slow shock, nor a fast shock. Rather, it provides a transition between the two. Therefore, it does not adhere to the e-Lax entropy condition (Lax 1957). This shock is admissible by the Liu entropy condition (Liu 1974, 1975):

$$\Lambda^{CD} \le \Lambda^{Di} , \qquad \forall \ i \text{ between } D \text{ and } C , \tag{11 a}$$

connecting the upstream state to the downstream state, and similarly on the downstream side of the shock:

$$\Lambda^{CD} \ge \Lambda^{Ci} , \qquad \forall \ i \text{ between } C \text{ and } D . \tag{11b}$$

Figures 12 and 13 show a graphical construction of the Liu entropy condition for the double contact discontinuity. By virtue of the concave downward curvature of the flux function between D and C along the C-tie line, this wave structure is stable.

3.4. Continuous Dependence of the Solution on Injection State
The solutions presented in this section focus on the nontie-line path that connects the injection tie line to the initial tie line. A graphical construction using fractional flow

theory demonstrates the conditions under which the double contact discontinuity occurs. The solution route presented in Figure 3 provides a transition between solutions that traverse the complete exterior branch of the nontie-line path and those that follow the complete interior branch of the nontie-line path (Figures 14 and 15). Type 1 utilizes the complete exterior branch of the nontie-line path traced from the initial tie line, A_1 to B_1, where A_1 is the equal-eigenvalue point of the initial tie line. A genuine shock along the injection tie line connects the nontie-line path to the injection composition. Figure 16 shows the graphical construction for this shock. The velocity of the genuine shock is given by the slope of the chord connecting B and I,

$$\Lambda = \frac{F_1^B - F_1^I}{C_1^B - C_1^I}. \tag{12}$$

The nontie-line eigenvalue, λ_{nt}^B, is represented by the slope of the line segment from B to π (Eq. 8 b). The shock on the injection tie line is a 1-Lax shock. As the injection gas saturation is decreased, the slope of $\overline{BI}$ steepens, the velocity of the genuine shock increases, and the length of the zone of constant state downstream of the shock decreases. The limit of this wave structure occurs when $I = I^*$. At this point, $\Lambda^{BI} = \lambda_{nt}^B$. Injection gas saturations below this value violate the velocity rule, and a new path must be found to connect injection and initial states.

Type 2 routes traverse the interior branch. They occur when the nontie-line path from I_2 is outside of the nontie-line path traced from A_1 (Figure 14). This solution route includes a nontie-line rarefaction from the injection composition to the initial tie line (I_2 to A_2) and a shock to the initial composition. At A_2, the landing point of the nontie-line rarefaction from I on the initial tie line, a zone of constant state separates the slow wave (I_2 to A_2) and the fast wave (A_2 to O). The limit of this solution occurs when the nontie-line path traced from the injection condition exactly matches the equal-eigenvalue point on the initial tie line (A_1). The saturations where these transitions occur depend on phase behavior and mobility ratio. Under these conditions, the zone of constant state collapses to a single point. Construction of this type of solution is initiated at the injection tie line, which is the longest tie line, as opposed to traditional construction which always starts at the shortest key tie line (Monroe *et al.* 1990, Jessen *et al.* 2001, Orr 2007).

Type 3 contains elements of both Type 1 and Type 2 solutions. The geometric construction at the C-tie line is illustrated in Figure 17. The slopes of the line segments representing the double contact discontinuity $\left(\overline{CD}\right)$ and the nontie-line eigenvalues immediately upstream $\left(\overline{\pi D}\right)$ and downstream $\left(\overline{\pi C}\right)$ of the shock coincide. As the injection saturation is decreased, the velocity of the discontinuity increases and the location of the C-tie line moves closer to the initial tie line, creating a family of solutions that vary smoothly from the injection tie line to the initial tie line.

4. Extensions
In this section we show that similar composition paths occur in four-component systems and systems with adsorption. We demonstrate, therefore, that the presence of the double contact discontinuity is pervasive in multicomponent, two-phase flow systems.

4.1. Four-Component, Two-Phase Flow with Constant K-Values

A solution involving the double contact discontinuity in a four-component system is presented in Figures 18 and 19. We consider a N_2-CH_4-CO_2-C_{10} system, where a mixture of 0.28 CH_4 and 0.72 C_{10} is displaced by a mixture of 0.5 N_2 and 0.5 CO_2. Such a system is applicable in flue gas injection into an oil reservoir for CO_2 sequestration and enhanced oil recovery. When CO_2-rich gas mixtures are injected into an oil reservoir, a large fraction of the injection gas dissolves in the oil phase, and the remaining quasi-ternary displacement effectively models two-phase injection conditions. In this system $K_{N_2} = 8$, $K_{CH_4} = 3.5$, $K_{CO_2} = 2$, $K_{C_{10}} = 0.01$ and M = 0.067. Parameters were chosen to approximate reservoir conditions of 70ºC and 10 MPa.

Solution construction starts with the procedure outlined in Monroe *et al.* (1990) and by Jessen *et al.* (2001). The key tie lines are identified: injection, initial and crossover tie line, as is the shortest tie line. In this system, the crossover tie line is the longest tie line. Solution paths from the injection tie line to the crossover tie line and the initial tie line to the crossover tie line are constructed independently. At point E, a path switch from the landing point of the tangent shock (F to E) to the nontie-line path is taken. The nontie-line path is taken up to the C-tie line, at which point the *double contact discontinuity* along the tie line facilitates the switch from the interior path to the exterior nontie-line path (D to C). This is followed by a nontie-line rarefaction to the equal-eigenvalue point on the initial tie line (C to B). At point B there is a path switch from nontie-line path to tie-line path. The solution is completed by a tie-line rarefaction to A, followed by a shock to initial conditions (A to O).

4.2. Four-Component, Two-Phase Flow with Adsorption

Similar displacement behavior occurs in systems with adsorption. Such solutions are applicable to enhanced coalbed methane recovery and shale gas reservoirs where gas components adsorb and desorb from the solid surface as gas mixtures propagate through the reservoir.

When effects of equilibrium adsorption are included, the conservation equations become:

$$\frac{\partial}{\partial t}\left[\sum_{j=1}^{n_p}\varphi x_{ij}\rho_j S_j + (1-\varphi)a_i\right] + \frac{\partial}{\partial x}\sum_{j=1}^{n_p}x_{ij}\rho_j u_j = 0, \quad i = 1,\ldots,n_c, \tag{13}$$

where ϕ is the porosity, a_i is the amount of component i adsorbed on the solid phase per unit volume of rock, u_j is local flow velocity of phase j, and n_p is the number of mobile phases. For a more detailed explanation of the extension of MOC theory to systems with adsorption, refer to Zhu (2003) and Seto (2007).

Adsorption is described using the multicomponent extension to the Langmuir isotherm of Markham and Benton (1931),

$$\theta_i = \frac{B_i p_i}{1 + \sum_{j=1}^{n_c} B_j P y_j}, \quad i = 1,\ldots,n_c, \quad j = 1,\ldots,n_c, \tag{14}$$

where the fractional coverage of individual components, θ, is a function of a Langmuir constant for a given temperature, B_i, for a pure gas species, P is the system pressure, and y_i is the equilibrium gas phase fraction of component i. In terms of molar concentration of adsorbed components, a_i, Eq. (15) is expressed as

$$a_i = \frac{\rho_i \rho_r V_{mi} B_i p_i}{1 + \sum_{j=1}^{N_c} B_j p_j}, \tag{15}$$

where ρ_r is the mass density of the coalbed, ρ_i is the molar density of component i at standard conditions and V_{mi} is the Langmuir constant at a specified temperature for component i. Adsorption constants and K-values used in this example are presented in Table 1. The mobility ratio for this system is 0.1.

Table 1: Summary of constants used in the example solution presented in Figure 20.

component	V_{mi} (scf/ton)	B_i (psi^{-1})	K
C_1	222	0.0017	5
C_2	444	0.0034	3
C_3	707	0.0066	1.2
C_4	0	0	0.1

To illustrate the double contact discontinuity in systems with adsorption, we consider displacement of initial composition 0.31 C_2 and 0.69 C_4 by a mixture containing 0.4 C_1 and 0.6 C_3. The composition path is presented in Figure 20. As in the example presented in the previous section, initial and injection segments are constructed independently. The solution route begins with a phase change shock from the injection composition, I, to the two-phase region. This is followed by a rarefaction along the injection tie line to point F. At F, a semishock connects the injection tie line with the crossover tie line. At the landing point on the crossover tie line of the injection segment, E, there is a path switch to the nontie-line path. A nontie-line rarefaction connects the crossover tie line with the C-tie line (E to D). This is followed by the double contact discontinuity that connects the injection segment to the initial segment (D to C). From point C, the nontie-line path is traced to the equal-eigenvalue point of the initial tie line, B, where there is a path switch from the nontie-line path to the tie-line path. This is followed by a rarefaction along the initial tie line to A and a tangent shock from A to the initial conditions, O, completes the composition path.

4.3. Four-Component, Two-Phase Flow with Composition Dependent K-Values and Adsorption

The simplified phase behavior representation of constant K-values has facilitated much of the geometric analysis and solution development for multicomponent MOC theory (Wang 1998, Johansen *et al.* 2005). Dindoruk (1992) demonstrated that this analysis holds when extended to an equation of state description of phase behavior. In this section, the initial assumption of constant K-values to evaluate component partitioning between aqueous and gaseous phases is relaxed. The Peng-Robinson equation of state (Peng and Robinson 1976) was used to evaluate phase densities. Thermodynamic parameters are summarized in Table 2. Values for adsorption parameters, V_{mi} and B_i, are the same as those summarized in Table 1, with C_1, C_2, C_3, and C_4 constants corresponding to N_2, CH_4, CO_2, and H_2O. A constant mobility ratio

was assumed (M = 0.054). Injection of a mixture of 0.5 N_2 and 0.5 CO_2 into a coalbed saturated with CH_4 and H_2O at 3000 kPa and 30ºC is considered, representing flue gas injection for enhanced coalbed methane recovery. For a more detailed development of the extension to the system presented here, refer to Seto *et al.* 2006.

Composition path is presented in Figure 21. Due to the low solubility of gases in the water phase and H_2O in the gas phase, the phase boundaries do not vary significantly. Composition paths are compressed towards the H_2O vertex. However, the solution structure remains the same. Due to the low solubility of H_2O in the gas phase, many pore volumes of CO_2 are required to vaporize all the H_2O in the coalbed. CH_4 recovery is determined by the nontie-line eigenvalue of the landing point of the crossover tie line (Seto *et al.* 2006, Seto 2007).

Table 2: Thermodynamic properties of components used in example solutions.

	P_c (kPa)	T_c (ºK)	ω	κ_{ij}			
				N_2	CH_4	CO_2	H_2O
N_2	3399	126.1	0.037	0	0.031	-0.02	0.275
CH_4	4599	190.6	0.011	0.031	0	0.103	0.491
CO_2	7377	304.1	0.224	-0.02	0.103	0	0.2
H_2O	22064	647.3	0.344	0.275	0.491	0.2	0

4.4 Discussion

We note finally that the presence of the additional C-tie line does not affect the technique developed by Wang and Orr (1997) for the analytical determination of minimum miscibility pressure. Miscibility occurs when one of the key tie lines is a critical tie line. The C-tie line is bounded by the crossover and initial tie lines. The size of the phase envelope decreases monotonically from crossover tie line to initial tie line. Of the three tie lines, the C-tie line will always have the intermediate length. Therefore, the C-tie line cannot be a critical tie line at pressure below that at which one of the other key tie lines is a critical tie line. Hence, the presence of the C-tie line does not change the minimum miscibility for injection of flue gas (a N_2/CO_2 mixture) for enhanced oil recovery in reservoir containing CH_4 and C_{10}, for example.

5. Conclusions

The occurrence of the double contact discontinuity in three-component, two-phase flows is demonstrated. This solution involves a path switch between two nontie-line paths by means of a double contact discontinuity along an intermediate tie line that is neither a 1-Lax shock, nor 2-Lax shock, but rather, a transition between the two. Stability of this structure is granted through adherence to the Liu entropy condition. This wave structure occurs under certain conditions of two-phase injection mixtures. The specific saturation at which it occurs is dependent on mobility ratio and phase behavior of the system. Construction of this solution requires identification of the C-tie line, resulting in a solution that requires n_c key tie lines to connect injection and initial states. Previous solutions involved only n_c-1 key tie lines. Additionally, solution construction is initiated at the longest tie line, whereas in previously investigated solutions, construction started with the shortest tie line. We have shown that this wave structure is stable and that it yields solutions that depend continuously on initial data. This solution provides the completes the set of building blocks for

solutions in the two-phase region, a necessary step for the development of a complete Riemann solver for three-component, two-phase flow.

We have also shown that the double contact discontinuity occurs in more general flows, like four-component systems with adsorption and composition-dependent K-values. Indeed, we anticipate that the wave structure presented here is a pervasive feature in multiphase compositional flows.

References

Berres, S., Burger, R.: On Riemann Problems and Front Tracking for a Model of Sedimentation of Polydisperse Suspensions. ZAMM **87** (10) 665-691 (2007)

Dafermos, C. M.: Hyperbolic Conservation Laws in Continuum Physics. Springer-Verlag, Berlin, Germany (2005)

Dindoruk, B.: Analytical Theory of Multiphase, Multicomponent Displacement in Porous Media. PhD dissertation, Stanford University, Stanford CA (1992)

Dindoruk, B., Orr, F. M. Jr., Johns, R. T.: Theory of Multicontact Miscible Displacement with Nitrogen. Soc. Pet. Eng. J. **2** (3) 268-279 (1997)

Falls, A. H., Schulte, W. M.: Features of Three Component, Three Phase Displacement in Porous Media. Soc. Pet. Eng. Reserv. Eng. **7** (4) 426-432 (1992)

Guzman, R. E., Fayers, F. J.: Solutions to the Three-Phase Buckley-Leverett Problem. Soc. Pet. Eng. J. **2** (3) 301-311 (1997)

Helfferich, F. G.: Theory of Multicomponent, Multiphase Displacement in Porous Media. Soc. Pet. Eng. J. **21** (2) 52-62 (1981)

Hirasaki, G. J.: Applications of the Theory of Multicomponent, Multiphase Displacement to Three-Component, Two-Phase Surfactant Flooding. Soc. Pet. Eng. J. **21** (4) 191-204 (1981)

Isaacson, E.: Global Solution for a Non-strictly Hyperbolic System of Conservation Laws Arising in Enhanced Oil Recovery. Rockerfeller University, *preprint* (1981)

Isaacson, E., Marchesin, D., Plohr, B., Temple, B.: Multiphase Flow Models with Singular Riemann Problems. Comp. and Appl. Math. **11** (2) 147-166 (1992)

Jeffrey, A.: *Quasilinear Hyperbolic Systems and Waves*. Pitman Publishing, London, UK (1976)

Jessen, K., Orr, F. M. Jr.: Gas Cycling and the Development of Miscibility in Condensate Reservoirs. Soc. Pet. Eng. Reservoir Evaluation and Engineering **7** (5) 334-342 (2004)

Jessen, K., Wang, Y., Ermakov, P., Zhu, J., Orr, F. M. Jr.: Fast, Approximate Solutions for 1D Multicomponent Gas-Injection Problems. Soc. Pet. Eng. J. **6** (4) 442-451 (2001)

Johansen, T., Winther, R.: The Solution of the Riemann Problem for a Hyperbolic System of Conservation Laws Modeling Polymer Flooding. SIAM J. Math. Anal. **19** (5) 541-566 (1988)

Johansen, T., Wang, Y., Orr, F. M. Jr., Dindoruk, B.: Four-component gas/oil displacements in one dimension: Part I: Global triangular structure. Transp. Porous Media **61** (1) 59-76 (2005)

Johns, R. T.: Analytical Theory of Multicomponent Gas Drives with Two-Phase Mass Transfer. PhD dissertation, Stanford University, Stanford CA (1992)

Johns, R. T., Dindoruk, B., Orr, F. M. Jr.: Analytical Theory of Combined Condensing/Vaporizing Gas Drives. Soc. Pet. Eng. Advanced Technology Series **1** (2) 7-16 (1993)

Johns, R. T., Orr, F. M. Jr.: Miscible Gas Displacement of Multicomponent Oils. Soc. Pet. Eng. J. **1** (1) 39-50 (1996)

Juanes, R., Blunt, M.: Impact of Viscous Fingering on the Prediction of Optimum WAG Ratio. Soc. Pet. Eng. J. **12** (4) 486-495 (2007)

Juanes, R., Lie, K. –A.: Numerical Modeling of Multiphase First-Contact Miscible Flows. Part 2. Front-tracking/Streamline Simulation. Transp. Porous Media **72** (1) 97-120 (2008)

Juanes, R., Patzek, T. W.: Analytical Solution to the Riemann Problem of Three-Phase Flow in Porous Media. Transp. Porous Media **55** (1) 47-70 (2004)

Keyfitz, B., Kranzer, C.: A System of Non-strictly Hyperbolic Conservation Laws Arising in Elasticity Theory. Arch. Rat. Mech. Anal. **72** (3) 219-241 (1980)

LaForce, T., Jessen, K.: Analytical and Numerical Investigation of Multicomponent Multiphase WAG Displacements. paper SPE 110264 presented at the SPE Annual Technical Conference and Exhibition, Anaheim CA, November 11-14 (2007)

LaForce, T., Johns, R. T.: Effect of Quasi-Piston-Like Flow in Miscible Gasflood Recovery. paper SPE 93233 presented at the SPE Western Regional Meeting, Irvine CA, March 30-April 1 (2005)

LaForce, T.C., Jessen, K., Orr, F.M., Jr.: "Analytical Solutions for Four-Component Gas/Water/Oil Displacements: Part II, Example Solutions," Transp. Porous Media **72** (1) 83-96 (2008)

Larson, R. G., Hirasaki, G. J.: Analysis of the Physical Mechanisms in Surfactant Flooding. Soc. Pet. Eng. J. **8** (1) 42-58 (1978)

Lax, P. D.: Hyperbolic systems of conservation laws II, Comm. Pure Appl. Math. **10** 537-566 (1957)

Lie, K.-A., Juanes, R.: A Front-Tracking Method for the Simulation of Three-Phase Flow in Porous Media. Comput. Geosci. **9** 29-59 (2005)

Liu, T. -P.: The Riemann problem for general 2×2 conservation laws. Trans. Amer. Math. Soc. **119** 89-112 (1974)

Liu, T. –P.: The Riemann Problem for General Systems of Conservation Laws. J. Diff. Equations **18** (1) 218-234 (1975)

Marchesin, D., Plohr, B. J.: Wave Structure in WAG Recovery. Soc. Pet. Eng. J. **6** (2) 209-219 (2001)

Markham, E. C., Benton, A. F.: The Adsorption of Gas Mixtures by Silica. J. Amer. Chem. Soc. **53** 497-507 (1931).

Monroe, W. W., Silva, M. K., Larsen, L. L., Orr, F. M. Jr.: Composition Paths in Four-Component Systems: Effect of Dissolved Methane on 1D CO_2 Flood Performance. Soc. Pet. Eng. Res. Eng. **5** (3) 423-432 (1990)

Mota, J.: The Riemann Problem for a Simple Thermal Model for Two Phase Flow in Porous Media. Comp. and Appl. Math. **11** (2) 117-145 (1992)

Orr, F.M. Jr.: Theory of Gas Injection Processes, Tie Line Publications, Copenhagen (2007)

Orr, F. M. Jr., Johns, R. T., Dindoruk, B.: Development of Miscibility in Four-Component CO_2 Floods. Soc. Pet. Eng. Res. Eng. J. **8** (2) 135-142 (1993)

Peng, D. Y., Robinson, D. B.: A New Two-Constant Equation of State. Ind. Eng. Chem. Fund. **15** 59-64 (1976)

Seto, C. J.: Analytical Theory for Two-Phase, Multicomponent Flow with Adsorption. PhD dissertation, Stanford University, Stanford CA (2007)

Seto, C. J., Jessen, K., Orr, F. M. Jr.: A Multicomponent, Two-Phase Flow Model for CO_2 Storage and Enhanced Coalbed-Methane Recovery. Soc. Pet. Eng. J. **14** (1) 30-40 (2009)

Seto, C. J., Jessen, K., Orr, F. M. Jr.: Using Analytical Solutions in Compositional Streamline Simulation of a Field Scale CO_2 Injection Project. Soc. Pet. Eng. Res. Eng. Eval. **10** (4) 393-405 (2007)

Souza, A.: Stability of Singular Fundamental Solutions Under Perturbations for Flow in Porous Media. Comp. and Appl. Math. **11** (2) 73-115 (1992)

Souza, A.: Wave Structure for a Nonstrictly Hyperbolic System of Three Conservation Laws. Math. Comput. Modelling **22** (9) 1-29 (1995)

Wang, Y.: Analytical Calculation of Minimum Miscibility Pressure. PhD dissertation, Stanford University, Stanford CA (1998)

Wang, Y., Orr, F. M. Jr.: Analytical Calculation of Minimum Miscibility Pressure. Fluid Phase Equilibria **139** (1) 101-124 (1997)

Wang, Y., Dindoruk, Johansen, T., Orr, F.M. Jr.: Four-Component Gas/Oil Displacements in One Dimension: Part II: Analytical Solutions for Constant Equilibrium Ratios. Transp. Porous Media **60** (2005)

Zhu, J.: Multicomponent, Multiphase Flow in Porous Media with Temperature Variation and Adsorption, PhD dissertation, Stanford University, Stanford CA (2003)

Zhu, J., Jessen, K., Kovscek, A. R., Orr, F. M. Jr.: Analytical Theory of Coalbed Methane Recovery by Gas Injection. Soc. Pet. Eng. J. **8** (4) 371-379 (2003)
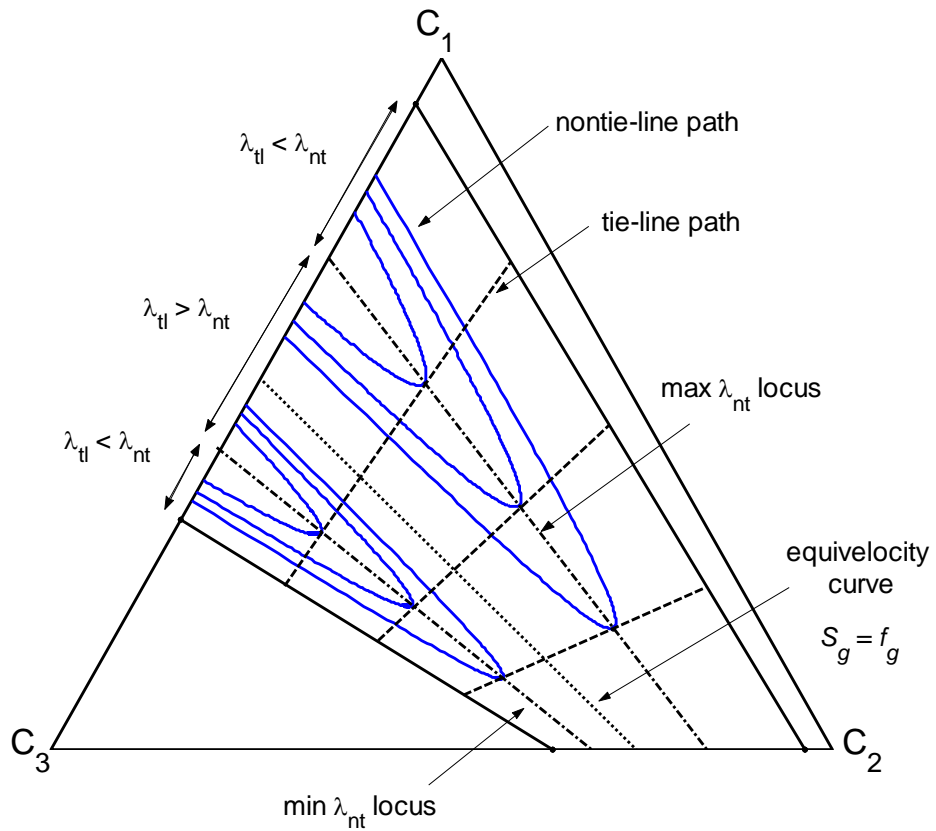
Figure 1. Tie-line and nontie-line paths in composition space. Tie-line paths are represented by the dashed line (--) and nontie-line paths are represented by the solid line (−).
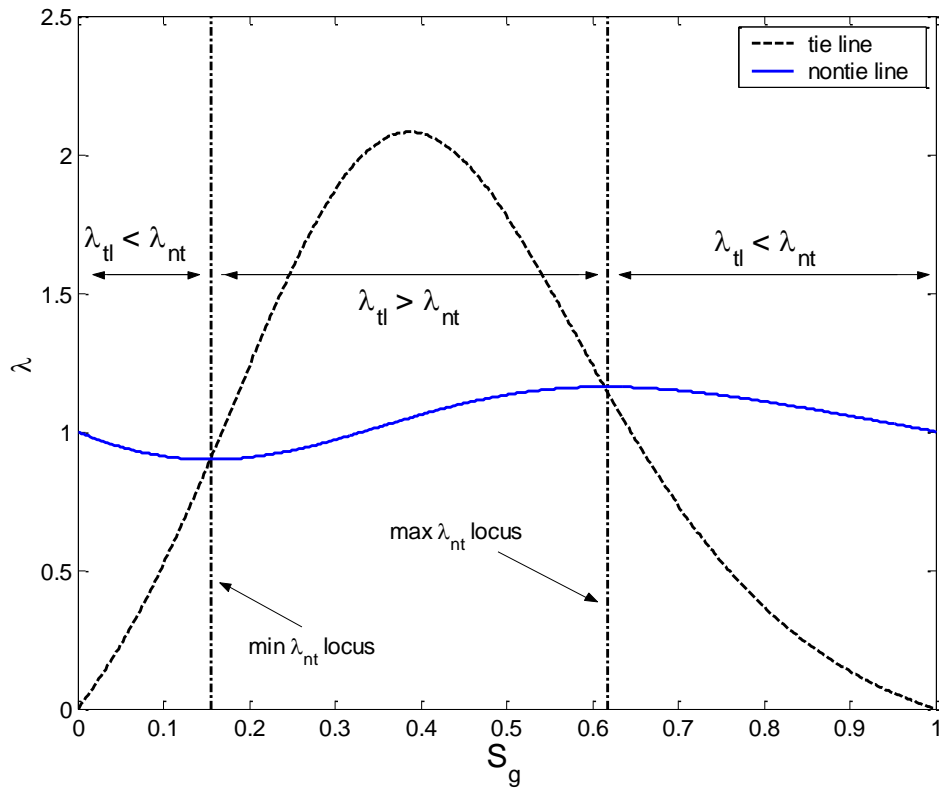
Figure 2. Evolution of tie line and nontie line wave velocities along a tie line. In the region bounded by the minimum and maximum λ_{nt}, λ_{tl} is the fast path, and λ_{nt} is the slow path. Outside of this region, the order of the wave velocities is switched.
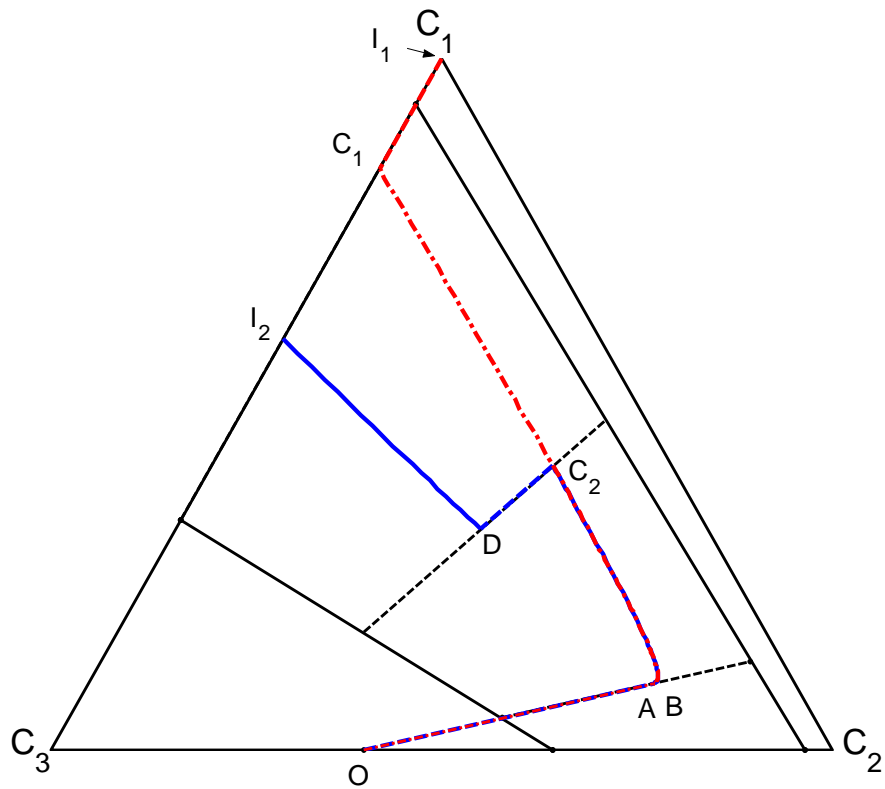
Figure 3. Composition path comparing the wave structure for single-phase injection (red) and the double contact discontinuity (blue) observed for some two-phase injection compositions.
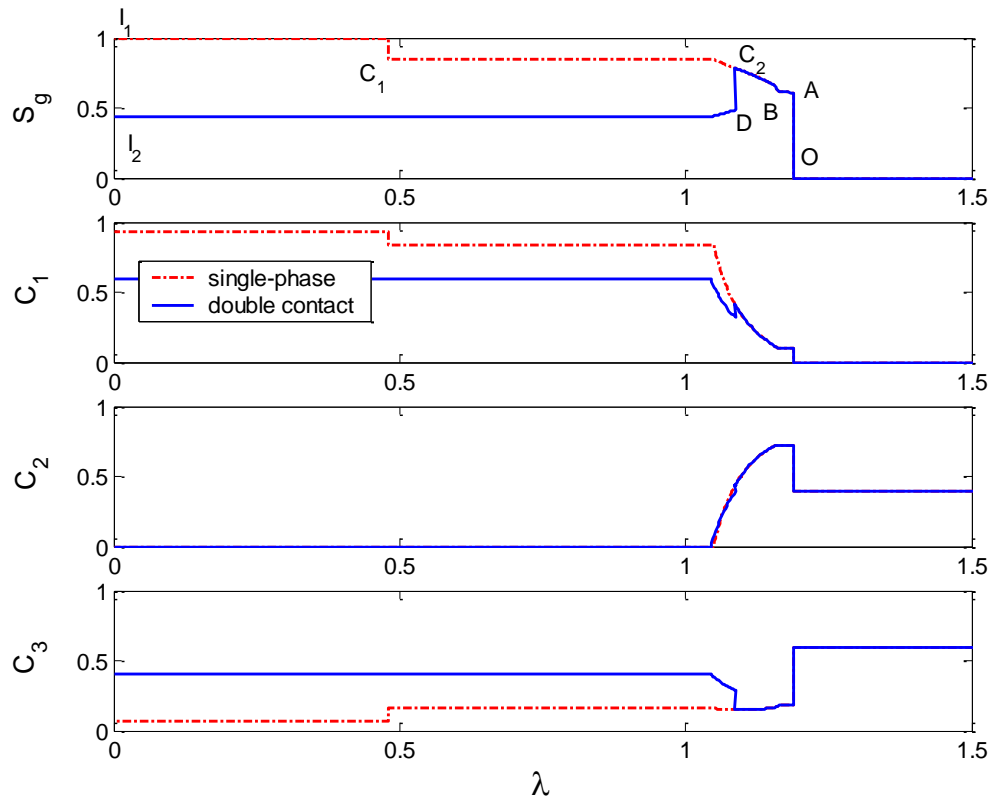
Figure 4. Solution profile corresponding to the composition path presented in Figure 3.
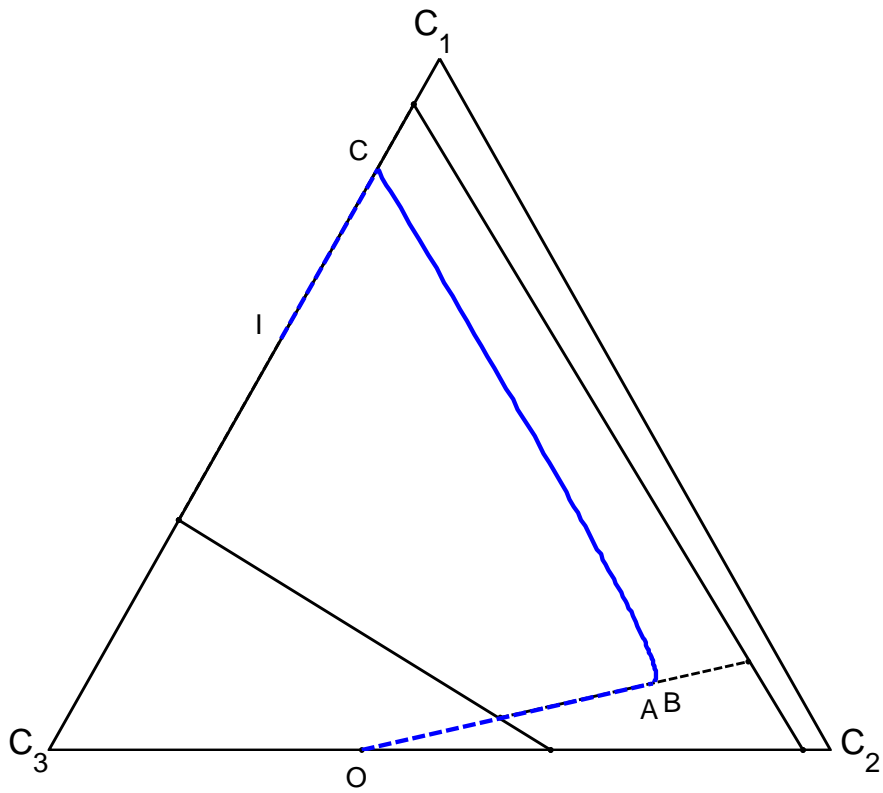
Figure 5. Composition path for Possible Solution 1: exterior nontie-line branch. The shock velocity from I to C is greater than the nontie-line eigenvalue at C.
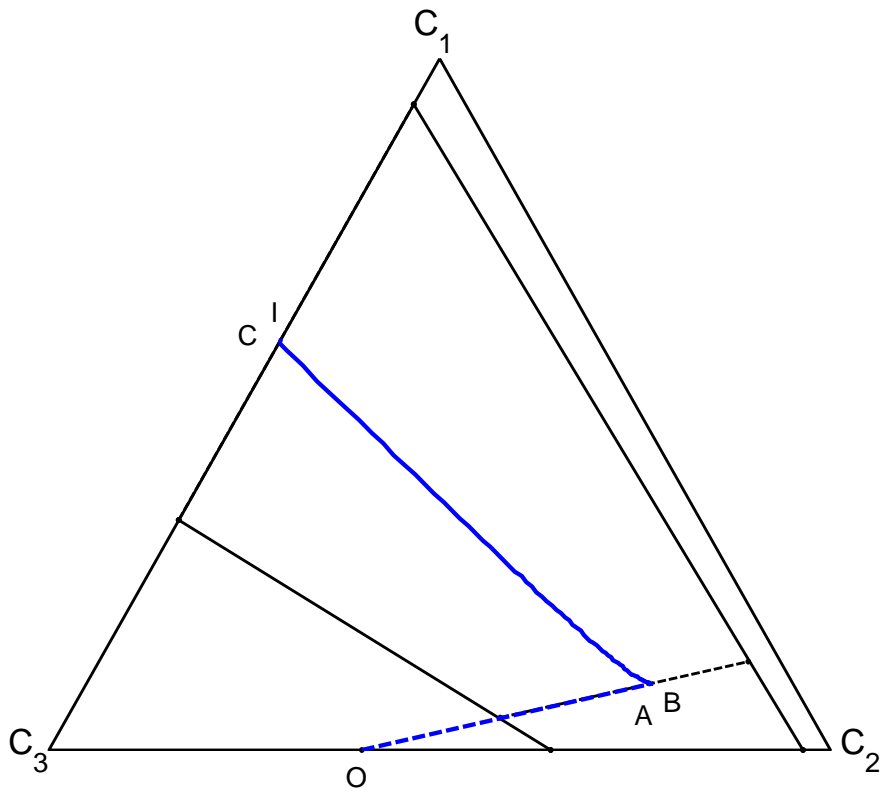
Figure 6. Composition path for Possible Solution 2: interior nontie-line branch. The shock velocity from I to C is greater than the nontie-line eigenvalue at C.
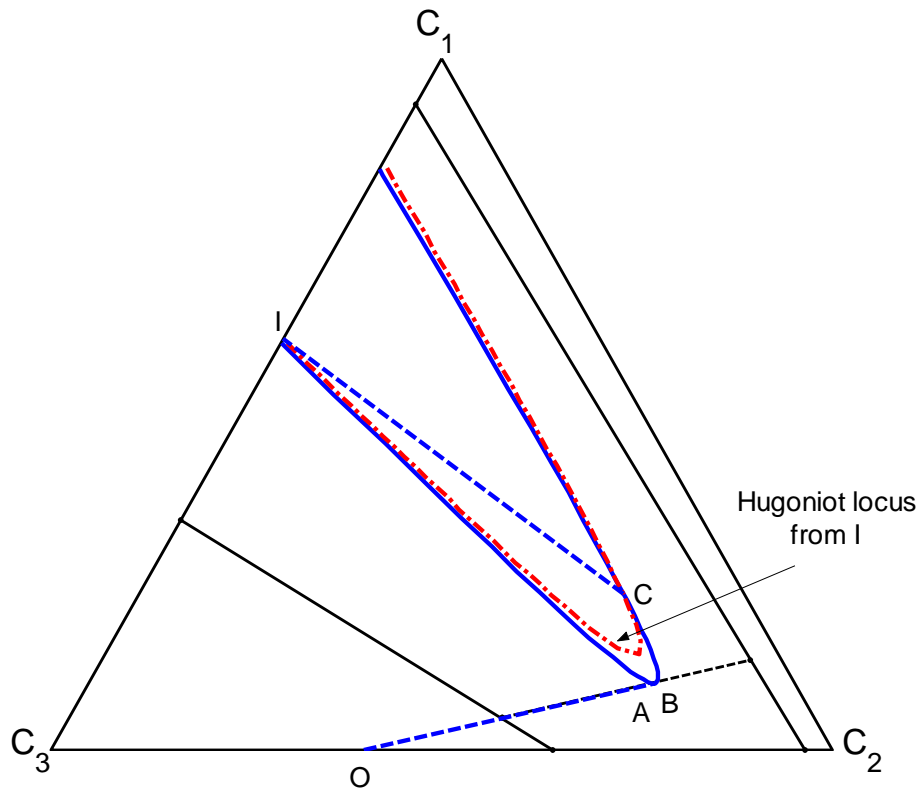
Figure 7. Composition path for Possible Solution 3: shock to nontie-line path. This shock from I to C does not satisfy the 1-Lax entropy conditions.
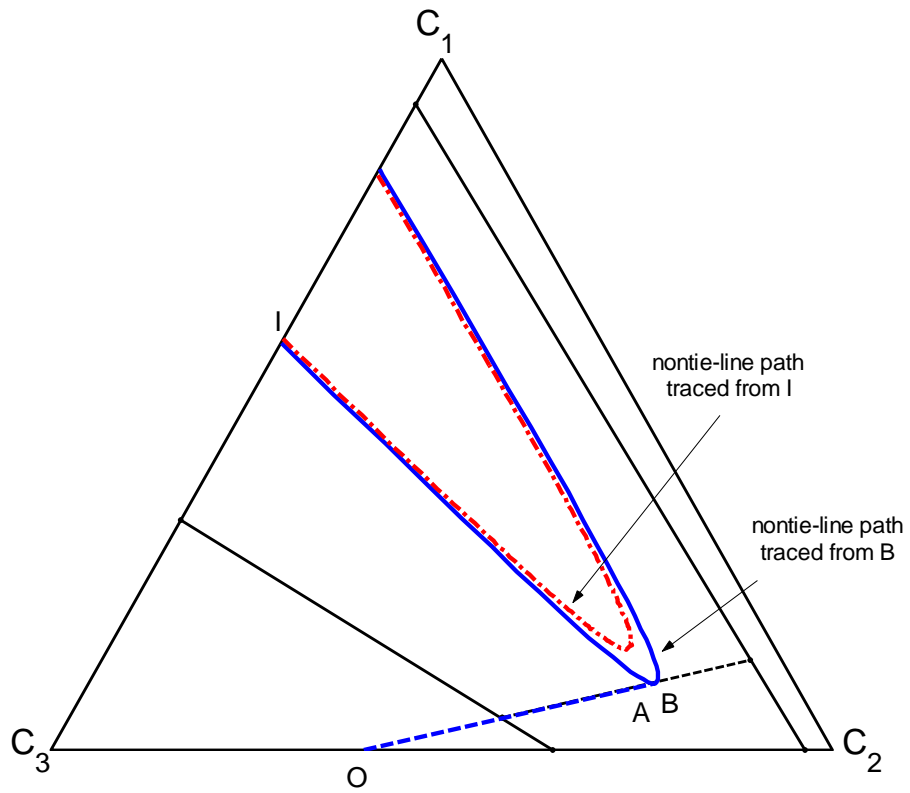
Figure 8. Composition path for Possible Solution 4: nontie-line rarefaction from point I. The nontie-line path does not intersect the initial tie line. Continuous variation to the initial tie line is not allowed.
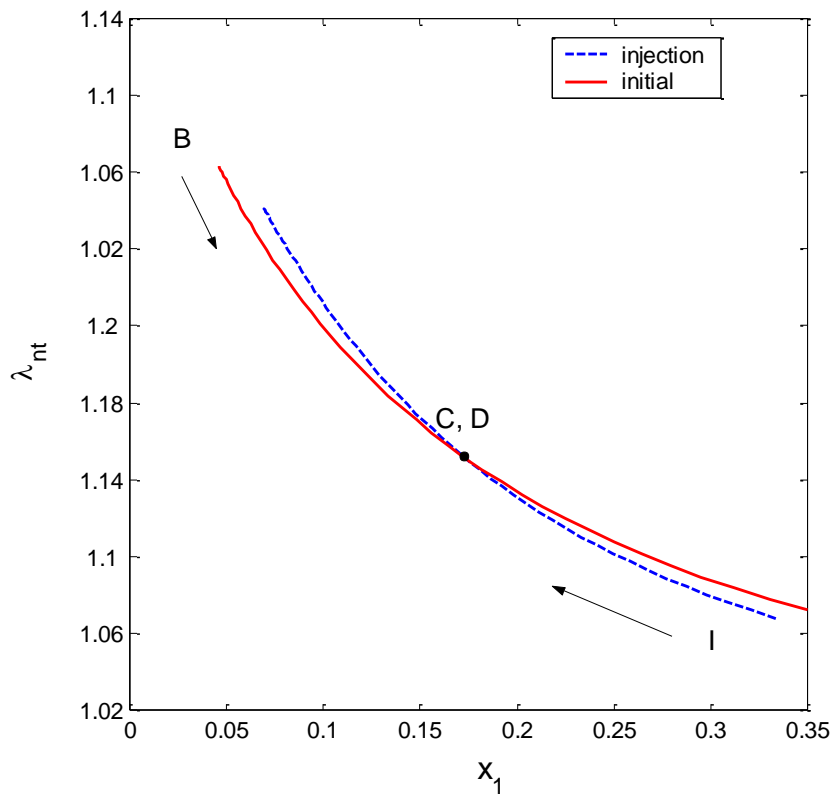
Figure 9. Injection and initial nontie-line wave velocities as a function of tie line traversed. A path switch from the injection tie line to the initial tie line is allowed along the tie line where the nontie-line wave velocities are equal.
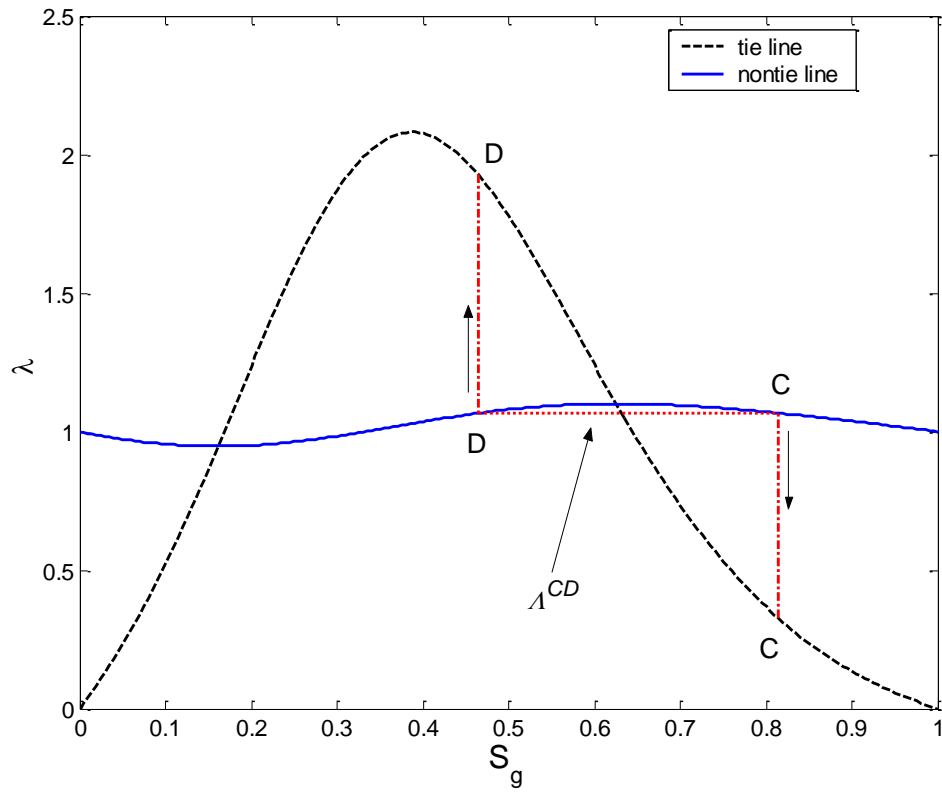
Figure 10. Path switches from the nontie-line paths to the contact tie line are permissible. However, continuous variation along the tie line, from D to C, violates the velocity rule. A shock from C to D, along the tie line, is required.
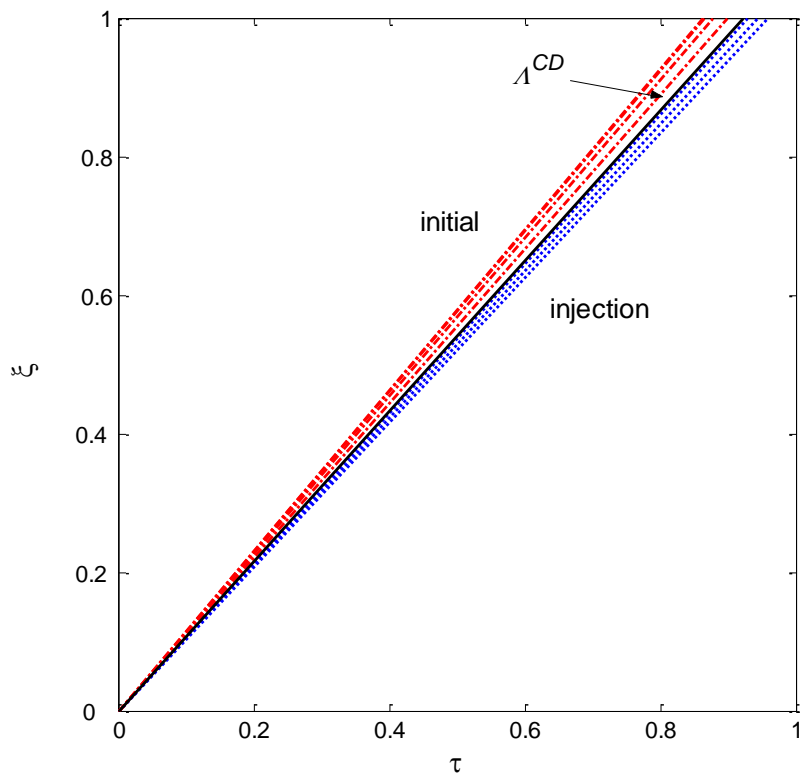
Figure 11. Development of characteristics along the permissible nontie-line path.
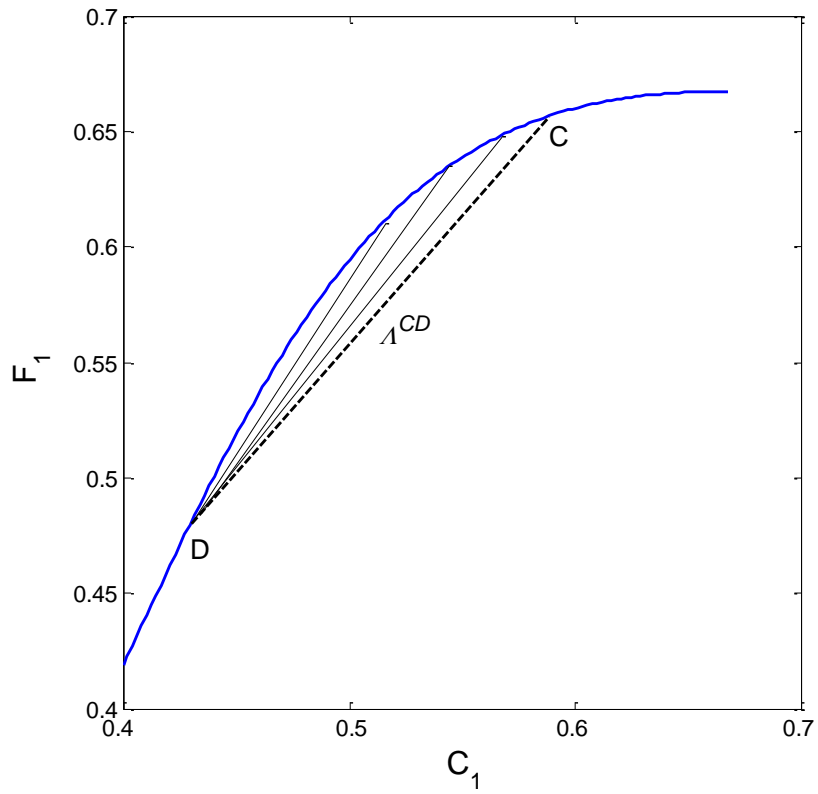
Figure 12. Stability of the double contact discontinuity connecting left state (D) to right state (C). Λ^{CD} is represented by the dashed line (--), and intermediate shocks from the upstream endpoint (D), Λ^{Di} are represented by the solid line (−).
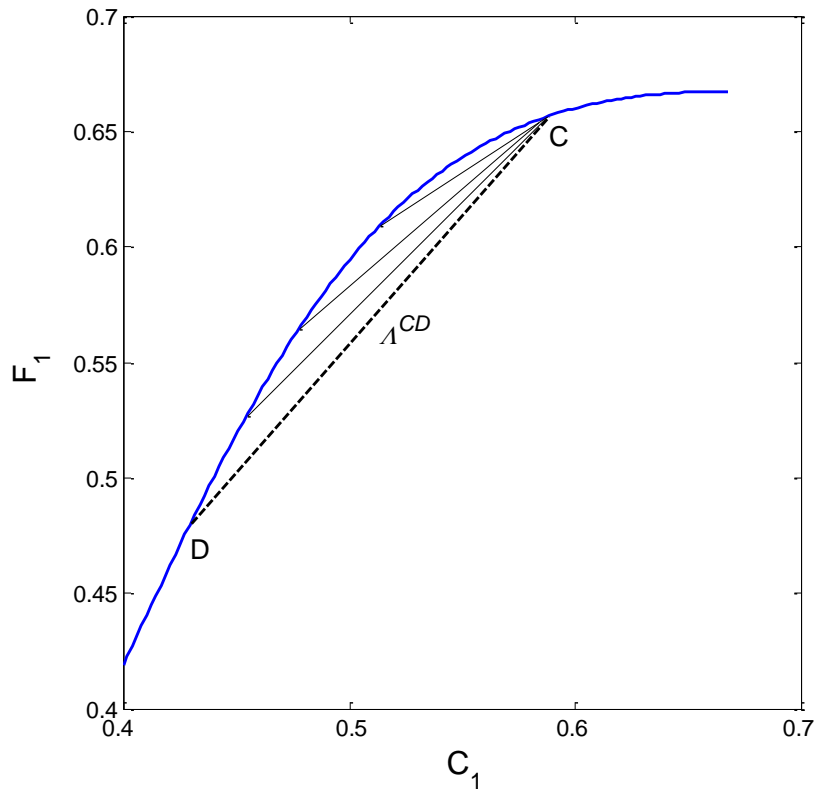
Figure 13. Stability of the double contact discontinuity connecting right state (C) to left state (D). $\varLambda^{CD}$ is represented by the dashed line (--), and intermediate shocks from the downstream endpoint (C), $\varLambda^{Ci}$ are represented by the solid line (−).
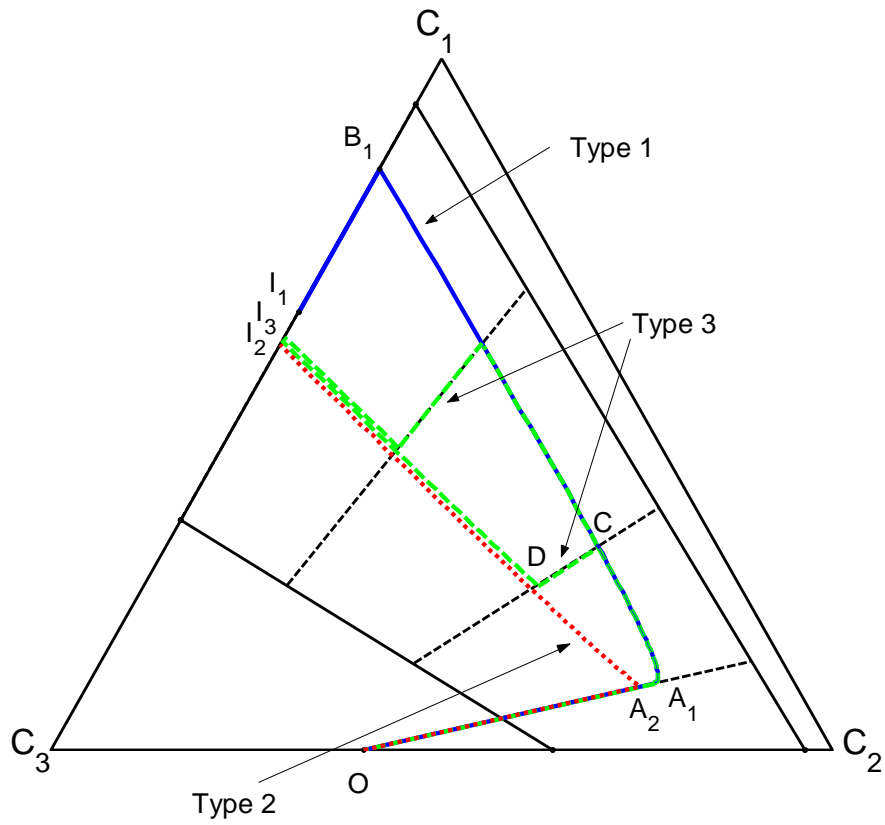
Figure 14. Composition paths demonstrating the transition from Type 1 solution to Type 2 solution through Type 3 solutions.
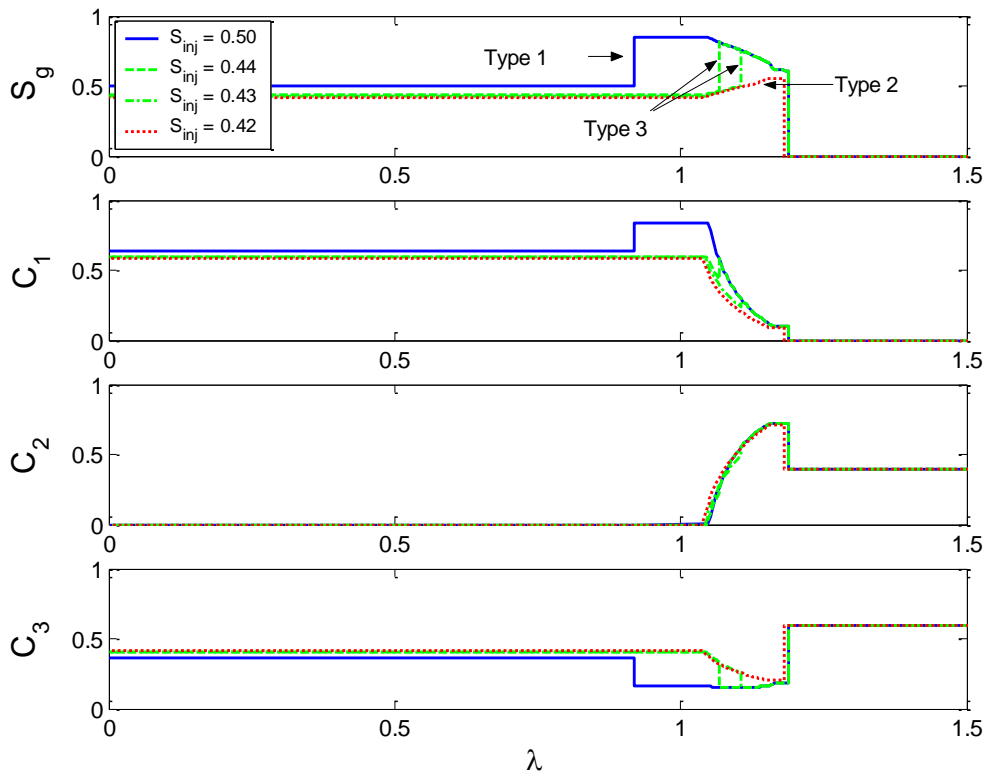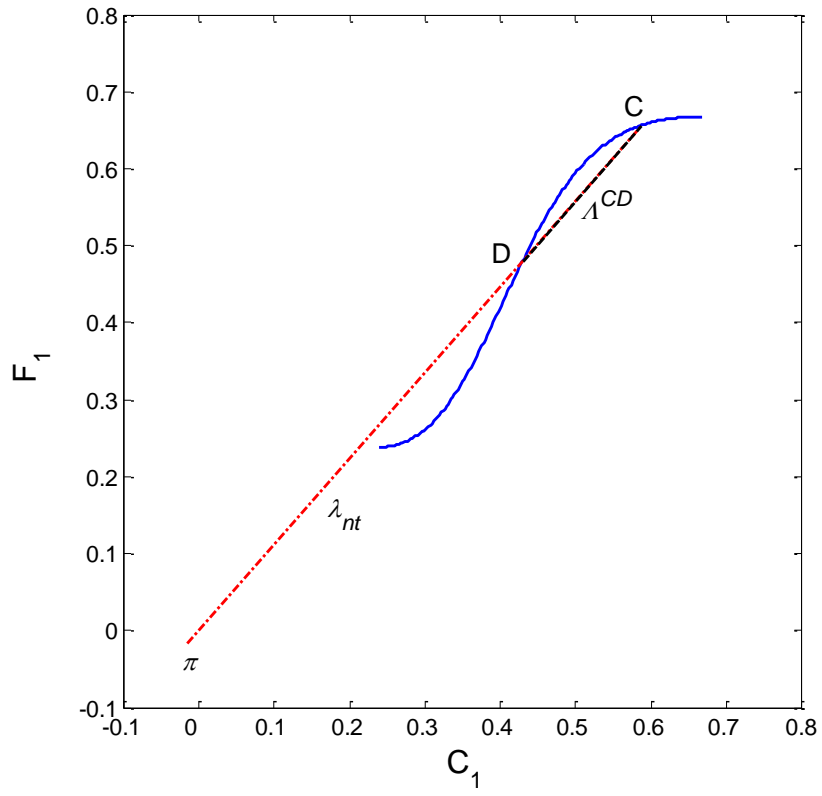
Figure 15. Solution profiles demonstrating the transition from Type 1 solution to Type 2 solution through Type 3 solutions.
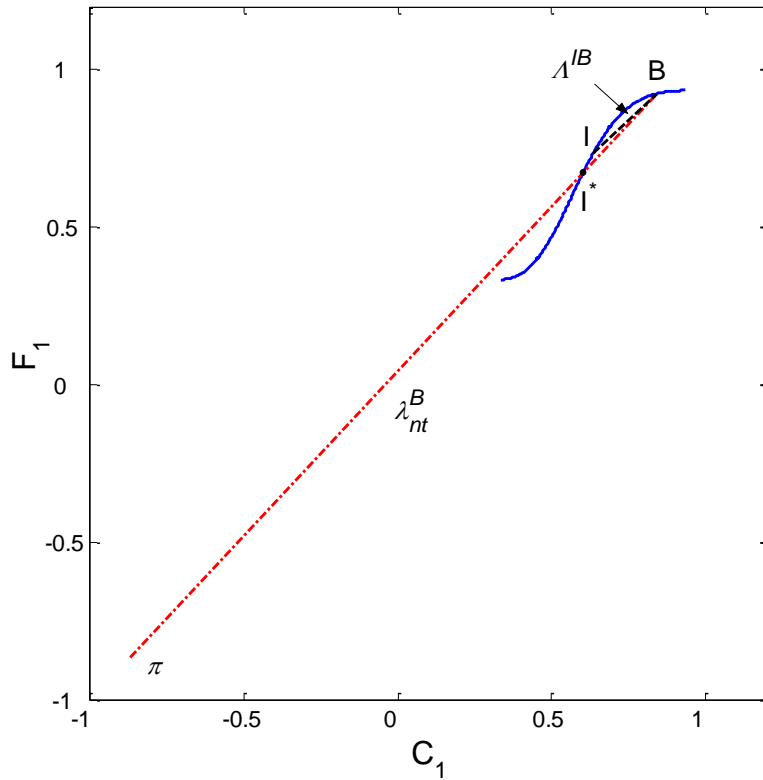
Figure 16. Graphical construction of Type 1 solution.

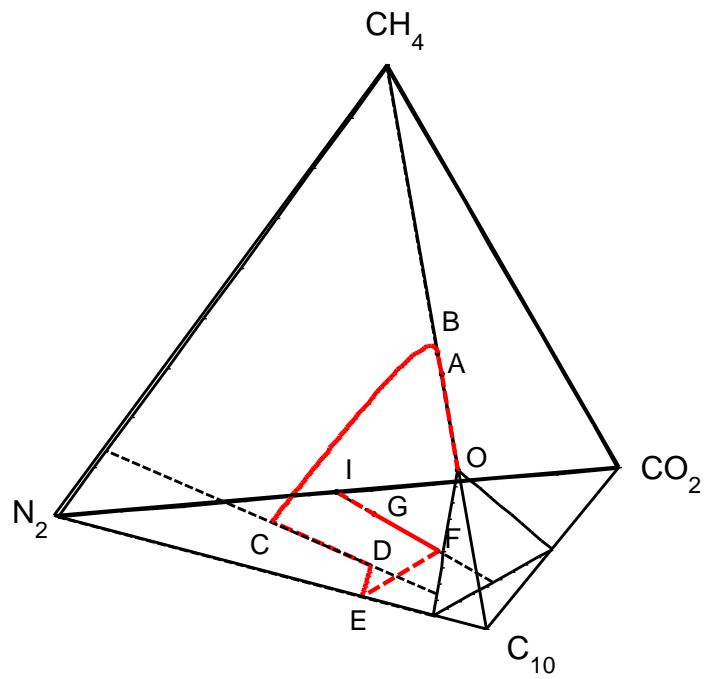Figure 17. Graphical construction of Type 3 solution.

Figure 18. Occurrence of a double contact discontinuity in a four-component, two-phase system with injection condition is single phase: $0.5 \, N_2$ and $0.5 \, CO_2$.
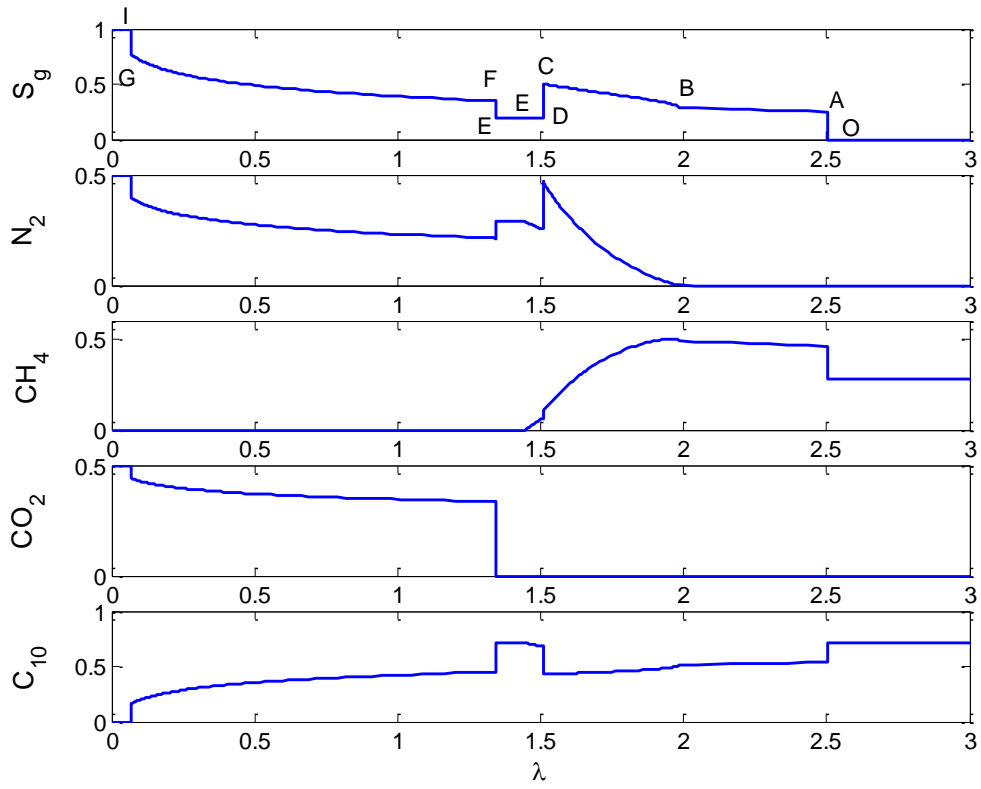
Figure 19. Solution profile showing the double contact discontinuity in a four-component, two-phase system.
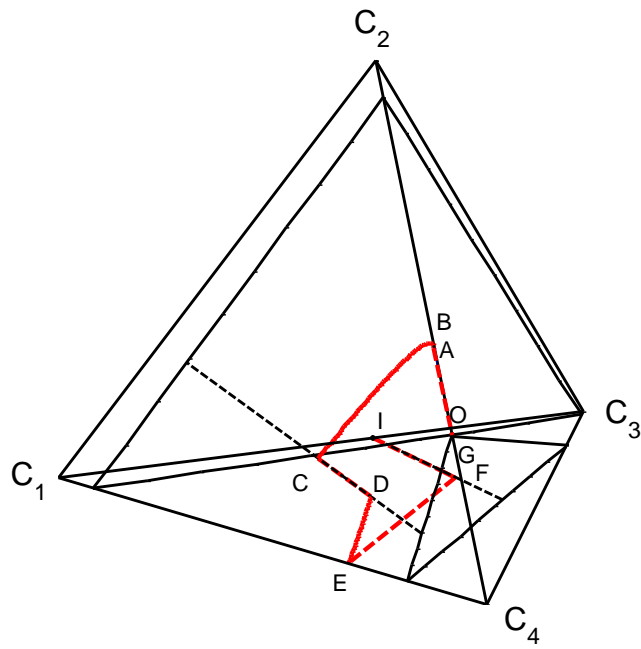
Figure 20. Extension of the four-component system to include adsorption. The double contact discontinuity also occurs in these systems.
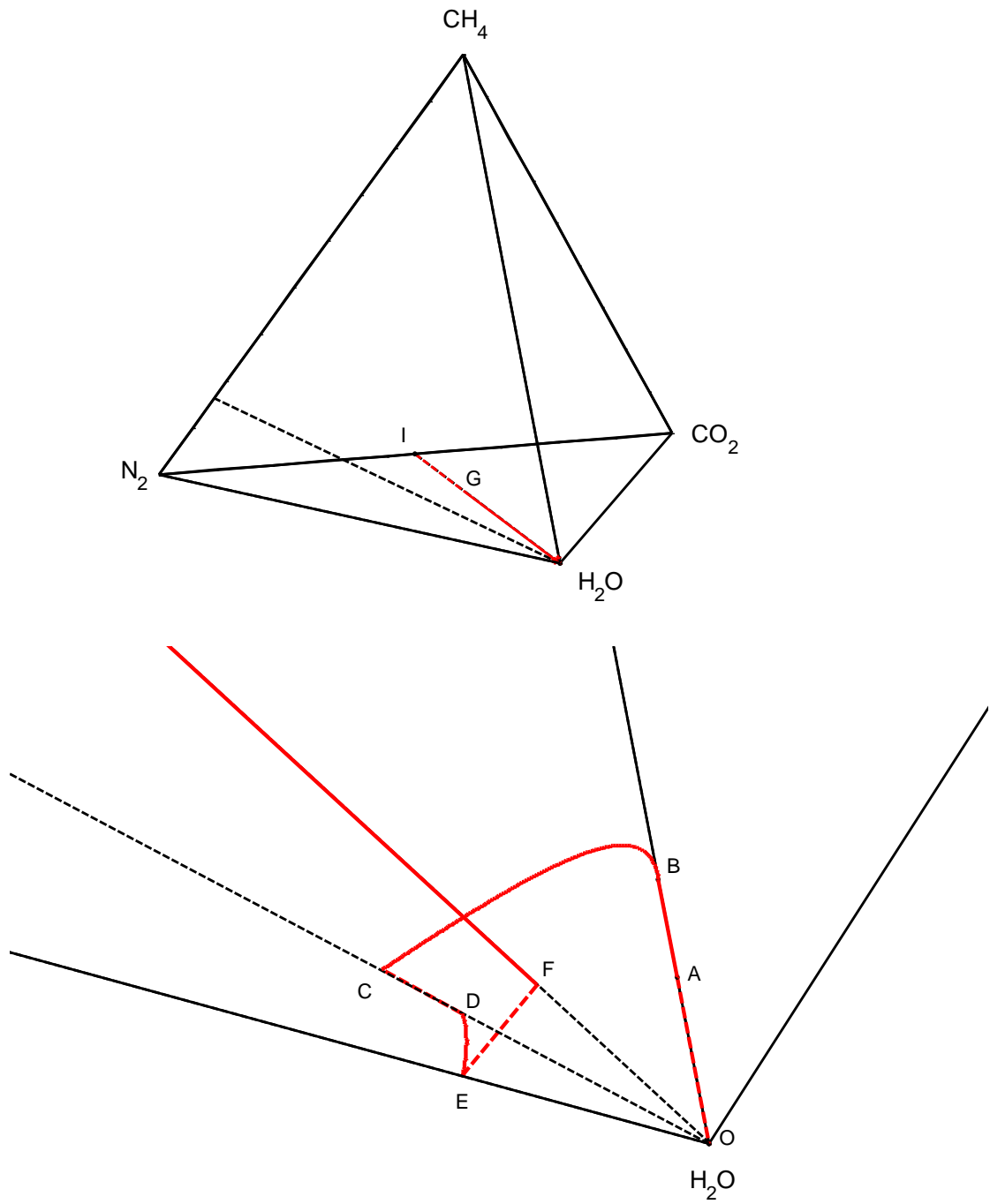
Figure 21. Extension of the MOC theory to include adsorption and composition dependent K-values. The full composition space is shown on the top. An enlargement of composition path at the H_2O vertex is shown on the bottom.